中華民國音響學會
第六屆學術研討會論文集

中華民國音響學會
行政院勞工委員會
行政院勞委會安衛所
行政院衛生署
行政院環境保護署
行政院環保署檢驗所
行政院環保署訓練所
台北市政府環境保護局

合辦

中華民國八十二年十二月四日

Hybrid Active and Passive Control for Structural Sound Radiation

Bor-Tsuen Wang

Department of Mechanical Engineering
National Pingtung Polytechnic Institute
Pingtung, Taiwan 91207

ABSTRACT

This paper analytically studies the hybrid active and passive control of sound radiation through a simply-supported beam mounted with an infinite rigid baffle. A harmonic point force is applied to the structure as the primary source (disturbance). A concentrated mass, a passive element, is added to the structure to restructure the modal properties. The piezoelectric actuator bonded to the structure surface is applied as the secondary source (control force), while the PVDF film is used as the near-field structural sensor. Active control is performed in conjunction with the use of LMS feedforward control algorithm. A minimization process is employed to calculate the optimal control voltage applied to the actuator. Both the passive element and active control are applied simultaneously and termed as the hybrid control. The radiated power verse excitation frequencies is plotted to evaluate the effectiveness of passive, active and hybrid control. Results show that active control can provide sufficient control for excitation near the resonance. With the proper selection of passive element, hybrid control can achieve better sound radiation control than passive or active control alone. This work demonstrates the feasibility to combine the active control mean and passive element applied to structural sound radiation control.

1. INTRODUCTION

Structural vibration and sound radiation control has been a great deal of interest. Ether passive or active control are generally applied to suppress the structural vibration so as to reduce the structural radiated sound. Passive noise control (PNC) is usually applied by adding mass, damping treatment or stiffening the structure [1,2]; however, PNC is generally inadequate and limited to low frequency noise control. Due to the development of fast processible personal computer, active noise cancellation methods have been drawn much attention. Steven and Ahuja [3] gave a good overview of active noise control (ANC). Upon the progress of sensor and actuator technology, the use of "smart", "adaptive" or "intelligent" structures involving distributed actuators, sensors and pc-based control algorithm can effectively control the sound radiation through vibrating structures. One of the frequently used distributed actuators and sensors is piezoceramic materials. The finite length of piezoelectric patch can be bonded to the surface of the structure and applied to induce or measure structural motion. Many works have been devoted to the applications of such a distributed actuator and sensor to vibration control of large structure [4-6] and to the control of structurally radiated noise [7-9].

Previous work by the author [10] applied piezoelectric actuators and accelerometers as error sensors in conjunction with the use of the concentrated mass, i.e., a passive control element, to perform hybrid structural vibration control. Results show that hybrid control performs better vibration control than passive or active control individually. This paper generally extracts this idea of hybrid active and passive control to attenuate the structurally radiated sound. A simply-supported beam mounted with an infinite baffled subjected to a harmonic point force is considered. A concentrated mass is added to the structure to passively reduce the structural motion and sound radiation as well. Active control is performed with the use of piezoelectric actuator and PVDF sensor in conjunction with the LMS feedforward control algorithm. Hybrid control is then applied by combining the passive control element and active control mean simultaneously. The radiated sound power verse excitation frequencies is shown to evaluate the effectiveness of passive, active and hybrid control. The beam displacement

distribution and radiation directivity are also shown to study the control mechanism as well as the wavenumber analysis. This work demonstrates that hybrid control can provide better acoustical control than active or passive control and also lead to providing an efficient way to the design of intelligent material structure system applied structural sound radiation control.

2. THEORETICAL ANALYSIS

2.1 Lateral Vibration of Uniform Beam

As shown in Figure 1, a concentrated mass, M, is located at x_M. The equation of motion can then be derived as follow:

$$E_b I\frac{\partial^4 w}{\partial x^4}+[\rho_b bt_b+M\delta(x-x_M)]\frac{\partial^2 w}{\partial t^2}=p(x,t) \tag{1}$$

where E_b is the Young's modulus of the beam; I the moment of inertia; ρ_b the beam density; t_b the beam thickness; b the beam width; $p(x,t)$ the force function. Note that the damping effect is assumed small and can be neglecHxd for simply application. The boundary condition for a simply-supported beam are

$$M(0,t)=M(L,t)=E_b I\frac{\partial^2 w}{\partial x^2}=0 \tag{2}$$

$$w(0,t)=w(L,t)=0 \tag{3}$$

To solve the above equation, Fourier Analysis with the eigenfunctions of homogeneous beam vibration forming the basis for spatial expansion will be performed [11]. The beam lateral displacement is assumed as follow:

$$w(x,t)=e^{i\omega t}\sum_{n=1}^{\infty} W_n \sin\alpha_n x \tag{4}$$

Here, the point force is applied as the disturbance input, and piezoelectric actuator is applied as the control input; therefore, the force function can be considered as the sum of both. By substituting the spatial expansion of beam lateral displacement Equation (4) into Equation (1) and applying the orthogonal properties of the eigenfunctions, the equation of motion is multiplied by $\sum_{m=1}^{\infty}\sin\alpha_m x$ and integrated over the beam, then the equation of motion become

$$\sum_{n=1}^{\infty}\sum_{m=1}^{\infty}\{W_n(\alpha_n^4-\frac{\rho_b bt_b}{E_b I}\omega^2)\frac{L}{2}\delta_{nm}-\frac{M\omega^2}{E_b I}W_n\sin\alpha_n x_M\sin\alpha_m x_M\}$$
$$-\sum_{m=1}^{\infty}\{\frac{F}{E_b I}\sin\alpha_m x_f+\frac{C_0\Lambda}{E_b I}\alpha_m(\cos\alpha_m x_1-\cos\alpha_m x_2)\} \tag{5}$$

The above equation can be rewritten in matrix form for the numerical solution purpose.

$$[R]_{m\times n}\{w\}_{n\times 1}=\{P\}_{m\times 1} \tag{6}$$

where [R], if m=n, is a symmetric modal coefficient matrix including both the beam stiffness and mass effect; {w} is the modal amplitude vector depending on the form of force function; {p} is the modal force vector which consists of the modal component of the point force disturbance and piezoelectric actuator. A typical element of [R], {w} and {P} can shown as follow:

$$R_{nm}=A_{nm}-\omega^2 B_{nm} \tag{7}$$

$$w_n=W_n \tag{8}$$

$$P_m=\frac{L}{2E_b I}(P_m^f+P_m^c) \tag{9}$$

where A_{nm}, B_{nm}, P_m^f and P_m^c are given in [10] and omitted for brevity. For free vibration analysis, Equation (6) can be reduced to the following form:

$$[A]\{w\}-\omega^2[B]\{w\} \tag{10}$$

One can easily solve the above generalized eigenvalue problem. Therefore, the natural frequencies of the beam with the concentrated mass can be obtained. To numerically solve Equation (6), Equation (6) can be decomposed into two independent linear system equations for both point force disturbance and piezoelectric actuator respectively as follow:

$$[R]\{w^f\}-\{p^f\}, \qquad [R]\{w^c\}-\{p^c\} \tag{11}$$

where $\{w^f\}$ and $\{w^c\}$ are the modal amplitude vectors for the point force and piezoelectric actuator which are to be determined; $\{p^f\}$ and $\{p^c\}$ are the modal force vectors for the point force and piezoelectric actuator. The modal amplitude vectors can then be determined by solving the above linear system equations. The beam lateral displacement due to the excitation of the point force and piezoelectric actuator can be obtained by substituting the corresponding modal amplitude vectors into Equation (4). Finally, the lateral displacement of the beam with a concentrated mass can be obtained by superposition method.

2.2 PVDF sensors' equations

For a PVDF film arranged as shown in Figure 1, the shape function can be expressed as follow:

$$\Gamma(x)-u(x-x_{s1})-u(x-x_{s2}) \tag{12}$$

where $u(x)$ is the step function; x_{s1} and x_{s2} are the coordinates of the PVDF film. The sensor's equation can then be derived as follows [12]:

$$q(t)-\frac{t_b+t_s}{2}b_s e_{31}\int_0^L \Gamma(x)\frac{\partial^2 w}{\partial x^2}dx \tag{13}$$

where b_s is the sensor width; t_s the sensor thickness; e_{31} the piezoelectric field intensity constant. By substituting $w(x,t)$ and integrating over the beam length,

$$q(t)-e^{i\omega t}(\frac{t_b+t_s}{2}e_{31}b)\sum_{n=1}^{\infty}\alpha_n W_n(\cos\alpha_n x_{s2}-\cos\alpha_n x_{s1}) \tag{14}$$

The generated voltages can then be expressed as:

$$V(t)-\frac{q(t)}{eA}t_s \tag{15}$$

where e is the permittivity of PVDF films; A is the sensor area. It is noted that the generated voltage is proportional to the slope difference between the two edges of a PVDF film.

2.3 Sound Radiated in the Far-Field

The far-field sound pressure radiated from a vibrating surface at a point in the acoustic field, as shown in Figure 2, is given by the Rayleigh integral [13]:

$$p(\vec{r},t)-\frac{i\omega\rho}{2\pi}\int_s \dot{w}(\vec{r}_s)\frac{e^{-ikR}}{R}ds \tag{16}$$

where $\vec{r}$ is the position vector of the observation point; $\vec{r}_s$ is the position vector of the elemental surface ds; $\dot{w}(\vec{r}_s)$ is the normal velocity of ds; R is $|\vec{r}-\vec{r}_s|$; ρ is the fluid density; and $k-\omega/c$ is the acoustic wavenumber. Here, the acoustic medium is air, and thus there is no feedback of the fluid motion into the structure. By substituting the beam velocity derived from Equation (4) into the Rayleigh integral, the sound pressure radiated to the far-field can be obtained [14]:

$$p(r,\theta,\phi,t)-e^{i\omega t}\sum_{n=1}^{\infty} W_n q_n \tag{17}$$

where

$$q_n = -i\omega \frac{\rho c b}{\pi} \frac{\kappa}{\alpha_n} \frac{e^{-ikr}}{2r} \left[\frac{1-(-1)^n e^{-i\alpha}}{1+(\alpha/n\pi)^2}\right]\left[\frac{1-e^{-i\beta}}{\beta}\right] \tag{18}$$

$$\alpha = \kappa L \sin\theta\cos\phi \tag{19}$$

$$\beta = \kappa b \sin\theta\sin\phi \tag{20}$$

Under the assumption of superposition, the total radiated sound pressure can be the sum of sound pressures due to the disturbance and control inputs

$$p_t = p_f + p_c = e^{i\omega t} \sum_{n=1}^{\infty} (W_n^f + W_n^c) q_n \tag{21}$$

The total radiated sound power defined as the integral of the square of the radiated sound pressure over the hemisphere of the radiating field can then be obtained:

$$\Phi_p = \frac{1}{2\rho c} \int_S |p_f|^2 dS = \frac{r^2}{2\rho c} \int_0^{2\pi} \int_0^{\pi/2} |p_f|^2 \sin\theta d\theta d\phi \tag{22}$$

The total radiated sound power can be an index to evaluate the effectiveness of sound radiation control.

2.4 Wavenumber Analysis

The beam velocity distribution can be taken Fourier integral transform in κ-plane.

$$\tilde{V}(\kappa_x, \kappa_y) = \int_{-\infty}^{\infty} \int_{-\infty}^{\infty} \dot{w}(x) e^{-i(\kappa_x x + \kappa_y y)} dx dy \tag{23}$$

where

$$\kappa_x = \kappa \sin\theta\cos\phi \tag{24}$$

$$\kappa_y = \kappa \sin\theta\sin\phi \tag{25}$$

therefore, the velocity transform can be expressed as:

$$\tilde{V}(\kappa_x, \kappa_y) = i\omega \sum_{n=1}^{\infty} W_n V_n \tag{26}$$

where

$$V_n = i\alpha_n \left[\frac{1-(-1)^n e^{-i\kappa_x L}}{\alpha_n^2 - \kappa_x^2}\right]\left[\frac{e^{-i\kappa_y b}-1}{\kappa_y}\right] \tag{27}$$

It is noted that the least mean square (LMS) value of the velocity transform, i.e., $|\tilde{V}|^2$, is proportional to the radiated sound power [13]. Only the wavenumber components satisfying $\kappa_x^2 + \kappa_y^2 < \kappa^2$ contribute to sound radiation into the far-field and are termed as supersonic waves. Others wavenumber components do not radiate into the far-field and are termed subsonic waves.

2.5 Cost Functions

For the use of N_s PVDF sensors, the cost function can be defined as the sum of the mean square voltages measured from the PVDF films:

$$\Psi_v = \sum_{j=1}^{N_s} |V_j|^2 \tag{28}$$

The linear quadratic optimal control theory (LQOCT) can then be applied to minimize the cost function so as to find the optimal control voltages input to the piezoelectric actuators. The full analysis can be referred to [15] and

omitted here for brevity. The vibrating energy of the beam can be expressed as follow:

$$\Phi_w = \int_0^L \dot{w}^2 dx \tag{31}$$

which can used as an index to evaluate the effectiveness of vibration control.

3. NUMERICAL RESULTS AND DISCUSSIONS

A steel beam with length of 0.38m, width of 0.04m, and thickness of 2mm is used in the simulations. The first few natural frequencies are 33.2 Hz, 128.8 Hz, 289.9 Hz, 515.4 Hz, 805.3 Hz and 1159.6 Hz. It is noted that no damping was included in the following analysis. The optimal process is suitable for controlling multiple primary sources; however, only one harmonic point force with input parameters, F=0.1N and x_f=0.067m, was considered for the following analysis. The piezoelectric patch (G-1195) [16] and PVDF films (LDT-28μk) [17] are respectively used. The piezoceramic patch is located at x_1=0.285m, x_2=0.3485m, and the PVDF film is located at x_{s1}=0.10m, x_{s2}=0.14m. The mass is assumed to be 50g. In order to calculate the beam response and radiated sound pressure, it was necessary to truncate the modal sums in Equation (4). Upon consideration of computing time and accuracy, the first 10 modes were considered, and it was found to provide sufficient convergence of series. Both the radiation directivity and beam displacement distributions were shown to demonstrate the control effectiveness of sound radiation through the beam. The radiated sound pressure is plotted in dB re 20×10^{-6} Pa over θ=-90° to 90°, while the beam displacement distribution is normalized by the largest amplitude in each case and plotted in dB along the beam length.

Figure 3 shows the total radiated power verse the excitation frequencies for applying passive control only. The arrangement of the concentrated mass, PVDF sensor and piezoelectric actuator is depicted on the top of the figure. The solid line denotes the radiated power due to the disturbance alone. Several peaks right on the resonance frequencies indicate the efficient radiation for on-resonance excitation. As the concentrated mass is added to the structure, the peaks have been shifted because the concentrated mass restructures the modal properties of the beam. For the case of M19, i.e., the mass is located at 0.19m in the center of the beam, the even resonance modes are not affected due to the symmetric location of the mass, and the odd resonance modes are shifted to the left. A few reduction of radiated power can be observed at low frequency ranges especially for off-resonance excitation. For the case of M13, i.e., the mass near the third mode nodal point, the third resonance mode is not changed, and the other resonance peaks are shifted. Again, a few reduction of radiated power can be observed at off-resonance frequencies for some low frequencies. Similar results can also be seen for the case of M07. Particularly, the radiated power is obviously attenuated for most off-resonance excitation below 1000Hz. With the proper selection of mass location, the resonance mode can be shifted to reduce the radiated power for on-resonance excitations of original system; however, spillover may occur at some off-resonance excitation frequencies. As the mass located away from the center of the beam, more reduction of radiated power can be achieved in the high frequencies ranges for off-resonance excitation.

Figure 4 shows the radiated power verse the excitation frequencies for the comparison of the passive, active and hybrid control. The arrangement of the system is shown on the top of the figure. For the passive control, i.e., the mass located at 0.07m, as discussed previously the resonance peaks are shifted due to the "restructuring" effect of the mass, and a few reduction of radiated power can be obtained for off-resonance excitation. Applying active control with the use of the piezoelectric actuator and PVDF sensor, the sound radiation can be well controlled for on-resonance excitation cases; however, little attenuation can be achieved for off-resonance excitation. A new resonance peak can also be observed near 330Hz. The reform of modal properties of the structure is due to the applied active control as discussed in [18]. As active and passive control applied simultaneously termed the hybrid control, similar results can be seen as those for active control except that hybrid control provides better sound radiation control for off-resonance cases. Therefore, with the proper selection of the active mean and passive element, hybrid control can provide better sound radiation control than either active or passive control applied individually.

Figure 5 shows the required control voltages applied to piezoelectric actuators verse excitation frequencies. The required control voltages are generally less than 25 volts sufficient for sound radiation control. As requiring high control voltages, the sound radiation control can not be achieved, and spillover occur. Figure 6 shows the similar plot as that in Figure 4 except the mass is located at 0.19m. Again, similar observations can be made as those found in Figure 4. It is noted that in contrast to that in Figure 4 little control can be achieved for off-resonance excitation near the fourth and fifth modes due to the improper location of the passive element.

To further study the control mechanism of passive, active and hybrid control, Figure 7 shows the beam displacement distribution, radiation directivity and the LMS of velocity transform for f=805Hz near the fifth resonance. The arrangement of the system is shown on the top of the figure. The solid line denotes the disturbance response and exhibits the fifth mode response for beam displacement distribution as shown in Figure 7(a). As shown in Figure 7(b), the radiation directivity pattern reveals the third mode response. This can be explained by Figure 7(c). Only the wavenumber components less than the acoustic wavenumber, termed supersonic region, can radiate. As the passive element applied, the beam displacement is globally reduced so are the radiated sound pressure and the LMS of velocity transform; however, the structural vibration and sound radiation characteristics of passive control are similar to those of the original system. With applying active control, the structural response is globally reduced and reveals the fourth mode, which is a less efficient radiated mode. The corresponding radiation directivity and the LMS of velocity transform are also globally attenuated and reformed as the dipole response. For hybrid control, further radiation of beam displacement and radiated sound pressure can be achieved. Again, with the proper selection of passive element incorporated with active control mean better structural sound radiation control can be obtained.

Figure 8 shows the similar results as in Figure 7 for f=129Hz near the second resonance mode. The mass is located at the center of the beam. As applying the passive control, no control can be achieved due to the mass located right on the nodal point of the second mode. For both active and hybrid control, structural vibration and sound radiation can be efficiently controlled. In particular, hybrid control can provide more attenuation of sound radiation than active control. It is noted that although the residual vibrating energy are close to 111 dB for both active and hybrid control, the residual radiated power for hybrid control is 13.7 dB less than that for active control. This can also be seen from the LMS of the velocity transform as shown in Figure 8(c), because the radiated power is proportional to the sum of the supersonic wavenumber.

4. CONCLUSIONS

This work has shown the feasibility of hybrid control combining the active control mean and passive control element to attenuate structural sound radiation. A simply-supported beam mounted with an infinite rigid baffle is assumed to be subjected to a harmonically excited point force. The concentrated mass, i.e., a passive control element, is added to restructure the modal properties of the beam so as to achieve sound radiation control; however, the control effectiveness is limited. Active control is performed with the use of the piezoelectric actuator and PVDF sensors to attenuate the structural sound radiation with the application of LMS feedforward control algorithm. Results show that active control can provide effective control for on-resonance excitation but not for off-resonance excitation. Hybrid control can achieve sufficient control for both on- and off-resonance excitation and provide better sound radiation control than active or passive control applied individually. Overall, hybrid control with the use of intelligent structure incorporated with passive control element can be an effective mean to attenuate structural radiated noise.

5. ACKNOWLEDGEMENTS

The author gratefully acknowledges the support of the work by National Science Council, Republic of China, under grant NSC82-0410-E-020-001.

6. REFERENCES

1. Vaicaitis, R., and M. Slazak, 1980, "Noise Transmission Through Stiffened Panel," Journal of Sound and Vibration, 70(3), pp. 413-426.

2. Koshigoe, S., and J. W. Murdock, 1993, "A Unified Analysis of Both Active and Passive Damping for a Plate with Piezoelectric Transducers," Journal of Acoustical Society of America, 93(1), pp. 346-355.
3. Stevens, J. C., and K. K. Aduja, 1991, "Recent Advances in Active Noise Control," AIAA Journal, 29(7), pp. 1058-1067.
4. Bailey, T., and J. E. Hubbard, Jr., 1985, "Distributed Piezoelectric-Polymer Active Vibration Control of a Cantilever Beam," Journal of Guidance and Control, 8(5), pp. 605-611.
5. Dimitriadis, E. K., C. R. Fuller, and C. A. Rogers, 1991, "Piezoelectric Actuators for Distributed Vibration Excitation of Thin Plates," Journal of Vibration and Acoustics, 113, pp. 100-107.
6. Wang, B. T., and C. A. Rogers, 1991, "Modeling of Finite-Length Spatially Distributed Induced Strain Actuators for Laminate Beams and Plates," Journal of Intelligent Material System and Structures, 2(1), pp. 38-58.
7. Wang, B.-T., E. K. Dimitriadis, and C. R. Fuller, 1991, "Active Control of Structurally Radiated Noise Using Multiple Piezoelectric Actuators," AIAA Journal, Vol. 29, No. 11, pp. 1802-1809.
8. Clark, R. L., C. R. Fuller, 1991, "Control of Sound Radiation with Adaptive Structures," Journal of Intelligent Material System and Structures, 2(3), pp. 431-452.
9. Clark, R. L., C. R. Fuller, 1992, "A Model Reference Approach for Implementing Active Structural Acoustic Control," Journal of Acoustical Society of America, 92(3), pp. 1534-1544.
10. Wang, B. T., 1992, "A Feasible Study of Hybrid Structural Vibration Control," The Proceedings of the Ninth National Conference of the Chinese Society of Mechanical Engineering, Kaohsiung, Taiwan, pp. 449-457.
11. Sandman, B. E., 1977, "Fluid-Loaded Vibration of an Elastic Plate Carrying a Concentrated Mass," Journal of Acoustical Society of America, 61(6), pp. 1503-1510.
12. Lee, C. K., and F. C. Moon, 1990, "Modal Sensors/Actuators," Journal of Applied Mechanics, 57(2), pp. 434-441.
13. Fahy, F., 1985, Sound and Structural Vibration, Academic, Orlando, Florida.
14. Wallace, C. E., 1972, "Radiation Resistance of a Baffled Beam," Journal of Acoustical Society of America, 51(3), pp. 936-945.
15. Wang, B.-T., 1992, "A Dynamic Simulation of Hybrid Active and Passive Control of Structural Vibration," NSC Report, NSC81-0401-E-020-501.
16. Piezo Systems, Inc., 1990, Product Catalog.
17. Pennwalt Corporation, 1990, Piezo Film Sensor Application Notes.
18. Burdisso, R. A., and C. R. Fuller, 1992, "Theory of Feedforward Control System Eigenproperties," Journal of Sound and Vibration, 153(3), pp. 437-452.

結構聲音輻射之混合主動與被動控制

王柏村
國立屏東技術學院
機械工程技術系

動被件源，主動、可達射被率控音輻時制動與元制制與被率控音動聲制控制估頻動聲主控為饋控評振被構合動作前動為激或結混被上方被作振動在之為構平將應共主制射塊結小若響近比控輻質於最，之接可動音中貼以壓率在制被聲集黏係電頻制控與的，器制制在控合動採源動控控量動混主支撐驅動佳能主，合簡干電主最射示件結障為壓，之輻顯元了屏構，器器音果動明體結質應動聲結被証剛於性感驅。，用文長用態構入制果選本限作模結輸控效當，無力之場算合制適制，有點構近計混控能控性。具振結為序為之如射行一諧變作程稱制，輻可討一改膜化用控制，音的探設可薄小作合控聲制文假構電最時混好之控本，結壓一同和良佳合制於以以制動到較混控加而，控主達到之

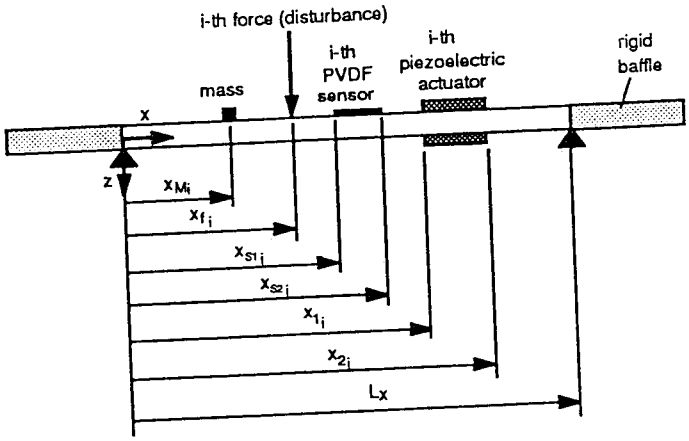

Figure 1. The arrangement and coordinates of simply-supported beam

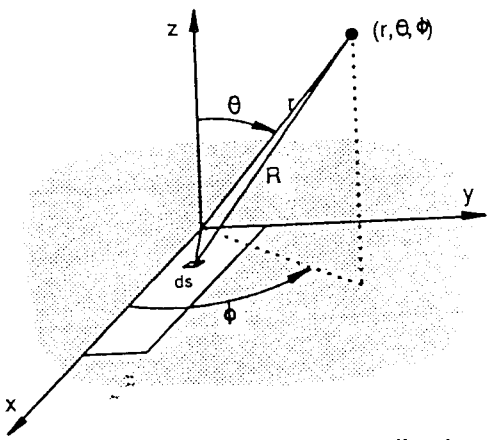

Figure 2. Sound radiated coordinates system

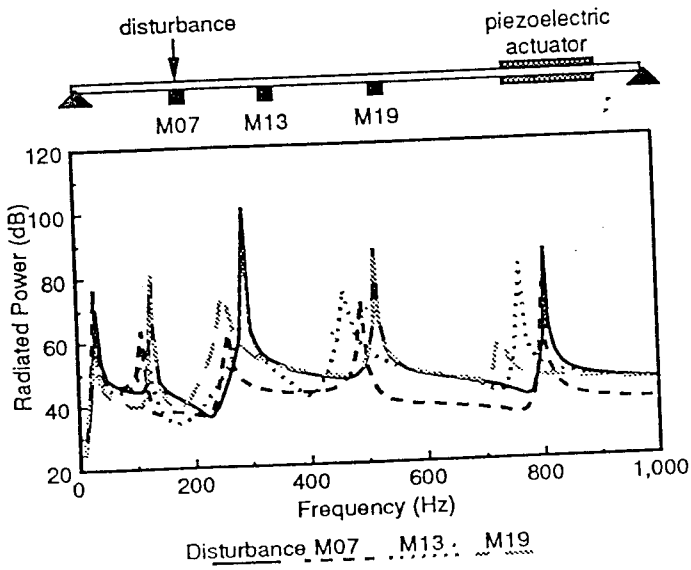

Figure 3. radiated power verse excitation frequencies for passive control

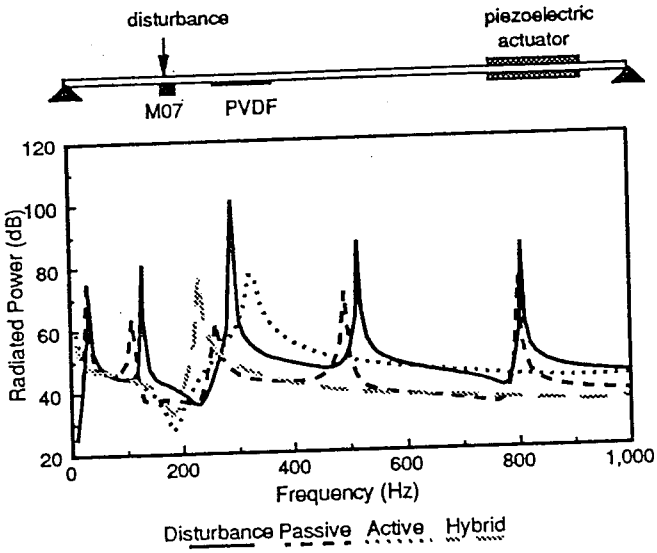

Figure 4. radiated power verse excitation frequencies for the comparison of passive (M07), active and hybrid control

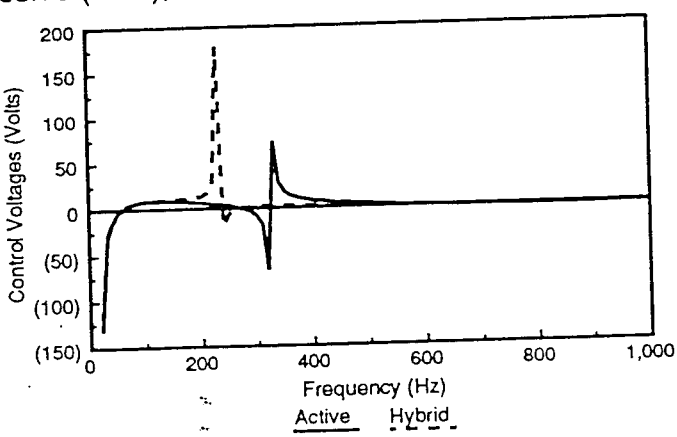

Figure 5. control voltages verse excitation frequencies for the comparison of active and hybrid control

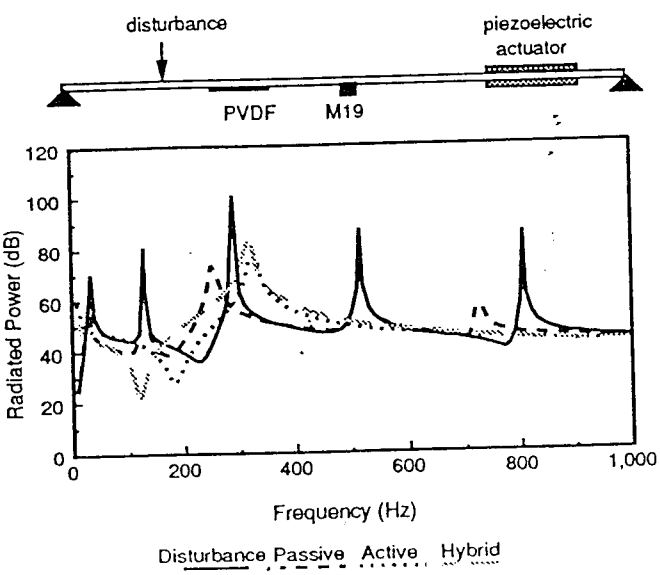

Figure 6. radiated power verse excitation frequencies for the comparison of passive (M19), active and hybrid control

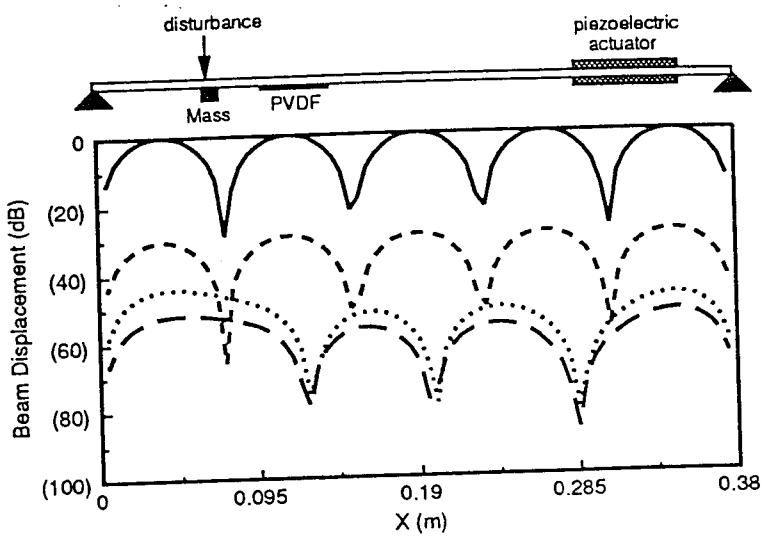

(a) beam displacement distributions

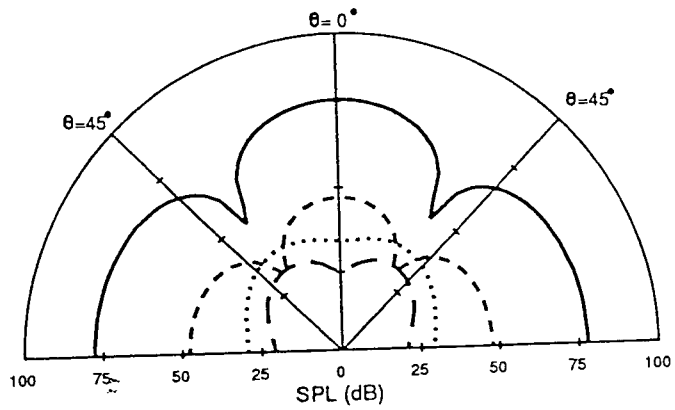

(b) radiation directivity

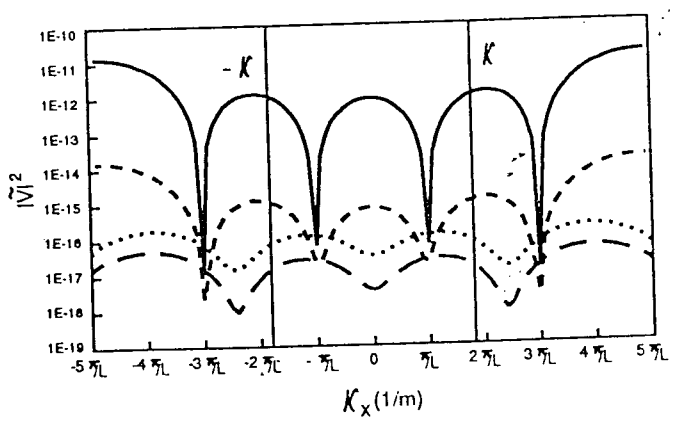

(c) LMS of velocity transform

	Disturbance	Passive	Active	Hybrid
vibrating energy (dB):	166.3	137.3	119.5	113.2
radiated power (dB):	85.4	55.2	43.2	35.5

Figure 7. A comparison of passive, active and hybrid control for f=805Hz

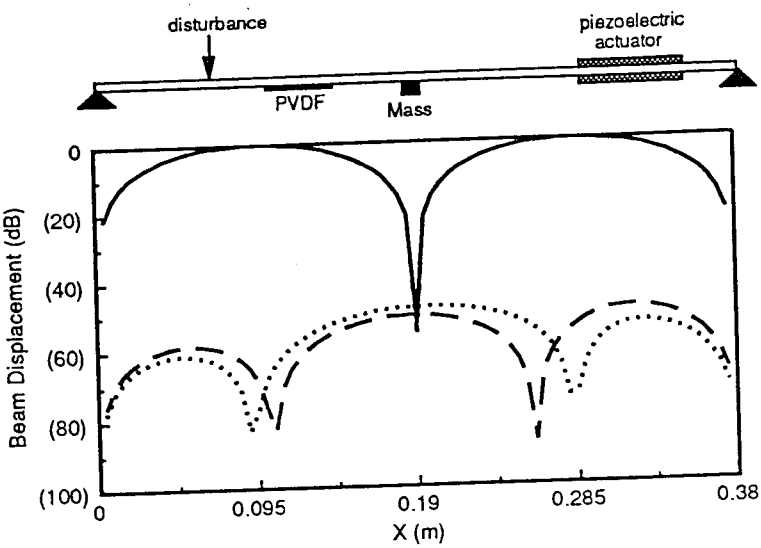

(a) beam displacement distributions

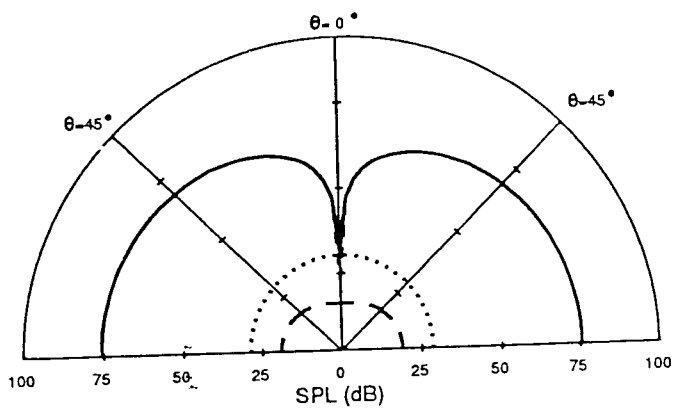

(b) radiation directivity

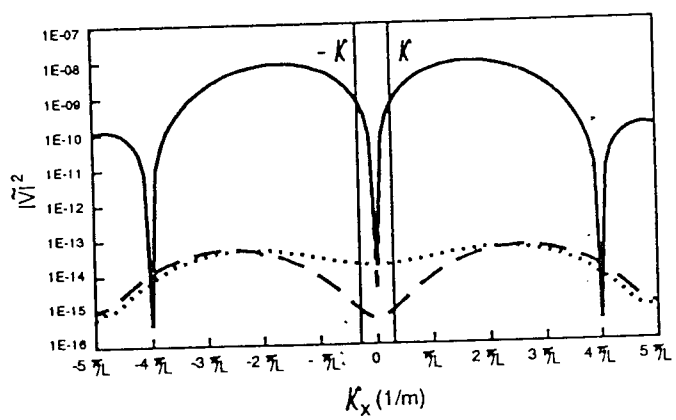

(c) LMS of velocity transform

	Disturbance	Passive	Active	Hybrid
vibrating energy (dB):	162.4	162.4	111.8	111.1
radiated power (dB):	80.9	80.9	41.8	28.1

Figure 8. A comparison of passive, active and hybrid control for f=129Hz